

Observation of Biochemical Imaging Changes in Human Pancreatic Cancer Tissue using Fourier-transform Infrared Microspectroscopy

Ying-Jen Chen, MD; Yih-Dih Cheng¹, PhD; Hsin-Yi Liu, MS²; Paul-Yann Lin³, MD; Chia-Siu Wang⁴, MD

Fourier-transform infrared (FT-IR) microspectroscopic mapping can be used to distinguish between different tissue structures, and to increase the image contrast between normal and cancerous regions of a given tissue sample. This study demonstrates the biochemical changes associated with a consistent link between cancerous tissue and various molecular changes in the IR spectra of human pancreatic cancer tissue using FT-IR mapping. Tissue samples were obtained immediately after resection in a patient who underwent a distal pancreatectomy including the pancreatic body and tail. The biochemical imaging changes of lipids, proteins, and nucleic acids in human pancreatic cancer tissue were analyzed via FT-IR microspectroscopy, using imaging, mapping, and line scan techniques. The intensities and frequencies of the absorption bands in the IR spectra of human pancreatic cancerous tissue were markedly reduced and shifted, particularly in the amide bands of protein and CH₂ and CH₃ stretching vibrations of lipids. The cancerous tissue contained significant protein content, and the distributions of DNA and lipid were very low, indicating low amounts of nucleic acids and lipids in human pancreatic cancer tissue. The analytical results indicate that these FT-IR microspectroscopic biochemical images reflect the distribution of cell components, which could be correlated with stained tissue in adenocarcinoma in pancreatic tissues. This study with samples of noncancerous and cancerous pancreatic tissues has clearly demonstrated that FT-IR microspectroscopy using the mapping method can be used for diagnosis. (*Chang Gung Med J* 2006;29:518-27)

Key words: pancreatic cancer, biochemical image, mapping, infrared microspectroscopy.

Pancreatic cancer remains a major public health problem in the United States and other developed countries. In the U.S. in 2004, it was estimated that 31,860 new cases of pancreatic cancer would be diagnosed, with 31,270 people dying from the disease.⁽¹⁾ Pancreatic cancer is the fourth leading cause of cancer-related death for both men and women, and is responsible for 6% of all cancer-related deaths.⁽¹⁾ In Taiwan, there were 35,201 cancer deaths

in 2003, accounting for 27% of all deaths. Pancreatic cancer was the tenth most prevalent cause of cancer-related deaths, being responsible for some 3% of all cancer-related deaths.⁽²⁾

Patients' survival depends on the extent of the disease and the performance status on diagnosis. The extent of disease is best categorized as resectable, locally advanced, or metastatic. Owing to diagnostic difficulties, the aggressiveness of pancreatic cancers,

From the Department of General Medicine, Chang Gung Memorial Hospital, Taipei; ¹Department of Pharmacy, ²Nursing Department, ³Department of Pathology, ⁴Department of Surgery, Chang Gung Memorial Hospital, Chiayi.

Received: Apr. 30, 2004; Accepted: Oct. 17, 2005

Correspondence to: Dr. Yih-Dih Cheng, Department of Pharmacy, Chang Gung Memorial Hospital, 6, West Section, Chia-Pu Road, Putz, Chia-Yi, Taiwan 613, R.O.C. Tel.: 886-5-3621000 ext. 2152; Fax: 886-5-3623002; E-mail: phdcheng@cgmh.org.tw

and a lack of effective systemic therapies, less than 5% of patients with adenocarcinoma of the pancreas generally survive more than five years following diagnosis.^(3,4) Current treatments are based on recent advances in studies of the molecular mechanisms involved in tumorigenesis. The precise interaction of the increasingly complex molecular alterations described to date in pancreatic carcinogenesis remains unclear. Novel therapies designed to correct molecular alterations may produce new treatment strategies and enhance understanding of the relative roles of these changes in pancreatic cancer biology. Numerous tumor-related antigens have been investigated in patients with pancreatic cancer. These substances are generally high-molecular-mass glycoproteins produced by either tumor cells or the surrounding tissues in response to the presence of tumors.⁽⁵⁾ This study uses FT-IR microspectroscopic mapping, imaging, and line scan techniques to observe the biochemical imaging changes and the chemical function distribution of protein bands in human pancreatic tissue.

IR microspectroscopic imaging techniques recently have been applied in various biological and medical studies, including cell visualization, detection of lipids, proteins, and nucleic acids, detection of polytene chromosomes in cells and tissue, and drug analysis of human hair.⁽⁶⁻⁸⁾ The applications of IR microspectroscopic mapping and imaging have also been extended to problems involving cellular structure and morphologic changes occurring in various diseased and cancerous tissues.⁽⁹⁻¹¹⁾ The strengths and adaptability of IR microspectroscopic imaging derive not only from the ability to determine chemical compositions and component distribution within a sample, but also from the ability to extract localized molecular information related to the sample architecture. For example, IR spectra are sensitive to changes in secondary and tertiary protein structure. Spectral shifts thus can be used to image the distributions of specific structural moieties within a biological sample, in contrast to simply measuring an overall distribution of a general class of molecules.

Since the IR spectra represent the fingerprint of a particular molecule, spectra from the image cube are used to uniquely and unambiguously identify sample components. Furthermore, biochemical IR microspectroscopic imaging also enables the identification and chemical distribution of cellular materials

and tissue components, information essential to understand biological activity. This study was the first to examine the biochemical imaging changes and protein conformational changes of human pancreatic cancer tissue, and observe the distribution of lipid, protein, and DNA in cancerous tissue using IR microspectroscopic imaging, mapping, and line scan analysis techniques.

CASE REPORT

Patient

A 51 year-old woman was diagnosed with cancer of the body and tail of the pancreas. On April, 2002, the patient received a distal pancreatectomy at Chang Gung Memorial Hospital - Chiayi. The pancreatic tissue measured $8 \times 2.7 \times 2$ cm. An ill-defined, firm tumor measuring $3.3 \times 2.2 \times 1.5$ cm was identified 0.5 cm away from the resection margin. Sections displayed moderately differentiated ductal adenocarcinoma of the pancreas with marked tissue desmoplasia and mild tumor necrosis. Extensive perineural invasion was also observed. There was focal tumor cell involvement in the resection margin of the pancreas. A peripancreatic lymph node with metastatic adenocarcinoma was observed.

Tissue preparation

Tissue samples were obtained immediately following resection. Sections were obtained from both the cancerous mass and noncancerous mass 5-10 cm away from the tumor, frozen in liquid nitrogen, and stored at -80°C until use. The frozen tissue was cut in a microtome at -20°C , and two 10- μm -thick sections were taken from each tissue sample. One tissue section was mounted on an aluminum foil-coated microscope slide for infrared microspectroscopic studies, while the other was fixed in formaldehyde, and stained with hematoxylin and eosin (H & E) for histological examination. The composition of each tissue section was scored blindly as a percentage of malignant and normal segments. This technique enabled close monitoring of the histological composition of each tissue section through spectroscopic examination.

Infrared spectral analysis

The infrared spectrum of the cancerous and noncancerous tissue was obtained using a Perkin-Elmer

Spectrum One FT-IR spectrometer (Perkin Elmer Ltd., Buckinghamshire, UK) equipped with a Perkin-Elmer AutoIMAGE IR microscope, a liquid nitrogen-cooled mercury-cadmium-telluride (MCT) detector and a zinc selenide attenuated total reflectance (ATR) prism. For each spectrum, 128 scans were performed at a spectral resolution of 4 cm^{-1} , with a normal range from 4000 to 700 cm^{-1} . For the microscopic mapping, a square region ($200 \times 200 \mu\text{m}$) of tissue was chosen and mapped using 10- μm steps in the X and Y directions (resolution 4 cm^{-1} , aperture 40 $\mu\text{m} \times 40 \mu\text{m}$, 16 scans). The second-derivative spectra were also used to confirm the peak positions and assignments of the IR spectra.

Infrared spectral characteristics of human pancreatic tissue

Human pancreatic cancerous and noncancerous tissues were determined by comparing with photomicrographs obtained from the hematoxylin-eosin-stained tissue. Fig. 1 illustrates the typical IR spectra of the cancerous and noncancerous tissue. The information contained in this IR absorption spectrum originates from many different types of biomolecules

in the tissue, including proteins, lipids, carbohydrates, and nucleic acids. Fig. 1 shows that the spectral patterns in the cancerous tissue differed from those in the corresponding noncancerous tissue. The most significant changes occurred in the absorbance regions from 3800 to 3100 cm^{-1} , 3100 to 2800 cm^{-1} , 1800 to 1500 cm^{-1} , and 1500 to 1200 cm^{-1} . Other changes could also be observed at a wavenumber between 1200 and 900. Particularly in the frequency region of the amide bands, the intensities of the amide A band, near 3296 cm^{-1} , and the amide B band, near 3085 cm^{-1} , in cancerous tissue were decreased owing to the N-H stretching vibration change in the peptide bond of the protein amide band compared with the noncancerous tissue.⁽¹²⁻¹⁴⁾ The intensity and frequency of the amide I band around 1659 cm^{-1} in cancerous tissue was reduced and shifted compared to noncancerous tissue, mainly owing to the C = O stretching vibration change in the protein backbones.⁽¹²⁻¹⁴⁾ Moreover, the intensity and frequency of the amide II band at around 1547 cm^{-1} in cancerous tissue were significantly reduced and shifted from noncancerous tissue, mainly owing to the N-H bending coupled with the C-N stretching

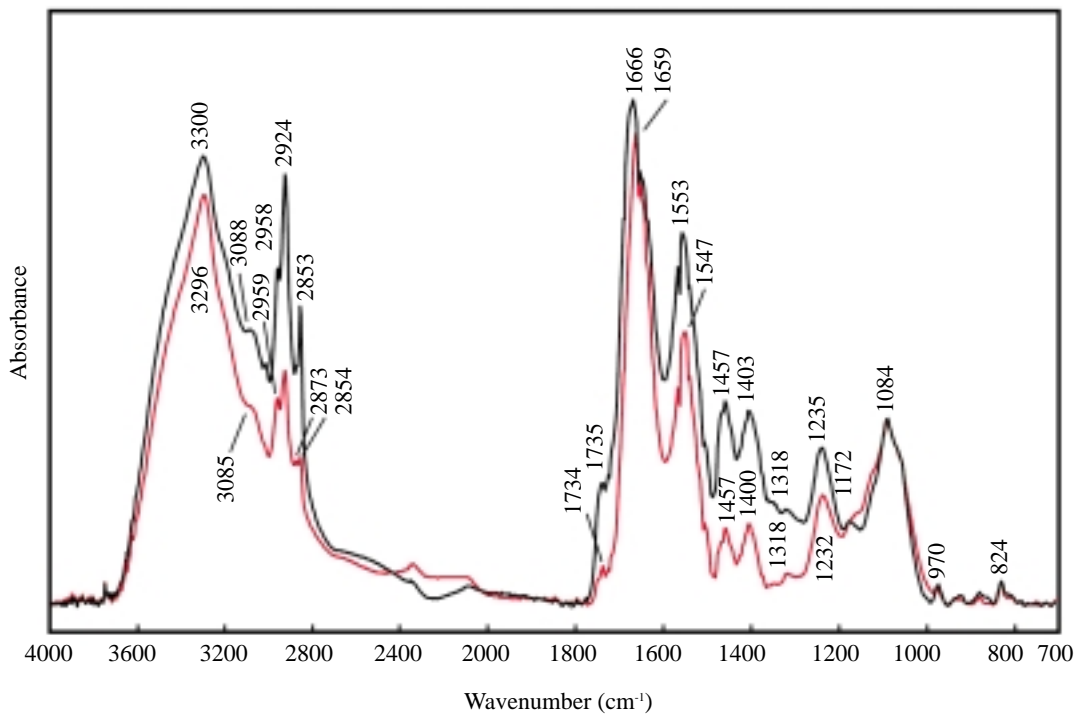


Fig. 1 Typical FT-IR spectra of noncancerous tissue (black line) and cancerous tissue (red line) in the human pancreas.

mode changing the peptide bond.⁽¹²⁻¹⁴⁾ The intensity of the amide III band in noncancerous tissue was also significantly reduced in cancerous tissue, and the frequency was shifted to 1232 cm^{-1} in cancerous tissue owing to the combination of changes in N-H bending and C-N stretching in the peptide group.⁽¹²⁻¹⁴⁾

The intensities of the absorption bands near 2959 and 2924 cm^{-1} in cancerous tissue were markedly decreased compared to the noncancerous tissue owing to C-H antisymmetric stretching of the CH_3 groups and $> \text{CH}_2$ groups of lipids, respectively.⁽¹³⁻¹⁴⁾ The intensities of the absorption bands at 2873 and 2854 cm^{-1} in cancerous tissue were also significantly decreased compared to noncancerous tissue owing to C-H symmetric stretching of the CH_3 groups and $> \text{CH}_2$ groups of lipids, respectively.⁽¹³⁻¹⁴⁾ The intensity of the absorption band at around 1734 cm^{-1} due to C = O stretching vibration of the carbonyl ester of phospholipids in cancerous tissue was gradually reduced in noncancerous tissue.^(11,13-15) Around 1232 cm^{-1} , superimposed bands typical of different $> \text{P} = \text{O}$ double-bond antisymmetric stretching vibrations of the phosphodiester free phosphate, and monoester phosphate functional groups in cancerous tissue were observed, and the intensity and frequency were reduced and shifted compared to the noncancerous tissue.^(11,13-16) Symmetric phosphate stretching vibration modes of the phosphodiester groups were also observed near 1084 cm^{-1} in cancerous tissue, while the intensity change was not obvious in noncancerous tissue.^(11,15,16) The absorption band at around 970 cm^{-1} in cancerous tissue resulted from the symmetric mode of dianionic phosphate monoesters of phosphorylated proteins and nucleic acids,^(14,16) and the intensity was slightly reduced compared to the noncancerous tissue. In cancerous tissue, the bands at 1457 and 1400 cm^{-1} were characteristic of the symmetric and antisymmetric CH_3 bending modes of methyl groups in proteins,^(14,16) and the intensity of both bands was significantly decreased compared to noncancerous tissue. A band at 1172 cm^{-1} appeared in cancerous tissue, corresponding to the C-O stretching mode of the C-OH groups of amino acid in cell proteins and to the C-O groups of carbohydrate,^(16,17) but it did not appear in noncancerous tissue.

Histological and infrared line scanning images of human pancreatic tissue

Fig. 2 shows the FTIR microscopic visible image of H & E stained pancreatic cancer tissue (Fig. 2A) and the infrared line scanning image of unstained cancer tissue (Fig. 2B). Fig. 2B illustrates that similar pathomorphological parts displayed similar spectral characteristics, indicating spatial biochemical homogeneity, and that different pathomorphological parts displayed heterogeneity in the cancer tissue. The intensities and frequencies of the absorbance bands changed markedly, particularly in the amide bands of protein and CH_2 and CH_3 stretching vibrations of lipids, reflecting differences in tissue structure differentiation. The changes in chemical function between the spectral features 3100 and 2800 cm^{-1} were dominated by absorption bands of the antisymmetric and symmetric C-H stretching vibrations of $-\text{CH}_3$ and $> \text{CH}_2$ methylene groups contained in fatty acids in cellular membranes.^(13,14) These vibrations could serve as sensitive monitors of the state-of-order of the membrane lipid matrix. The spectral region between 1800 and 1500 cm^{-1} was shaped mainly by the $> \text{C} = \text{O}$ stretching absorption band of ester carbonyl (near 1734 cm^{-1}) and the amide bands of the proteins.^(13,14) The conformational change of amide I band components noted between 1700 and 1600 cm^{-1} was conformation-sensitive, and could be used to differentiate the protein secondary structures α -helix, β -sheet, β -turns, and unordered structures.^(13,14) The amide II band between 1600 and 1500 cm^{-1} was more complex than the amide I band in the same region. The strongly absorbing amide II components of the α -helix and β -sheet components displayed perpendicular and parallel dichroism, respectively.^(13,14) Conformational change in amide III was also noted in the region of 1330 to 1200 cm^{-1} .^(13,14) Nucleic acids caused infrared absorptions between 1300 and 1000 cm^{-1} . Absorptions at approximately 1232 and 1084 cm^{-1} were generally attributed to stretching vibrations of the phosphodiester groups of the nucleic acids band.^(11,15,16) The position of these nucleic acid absorptions was sensitive to hydrogen bonding within the nucleic acids reflecting the nucleic acid structure.

Infrared mapping images of human pancreatic tissue

Although individual biochemical components have their own vibrational "fingerprints," including absorption bands with characteristic frequencies and

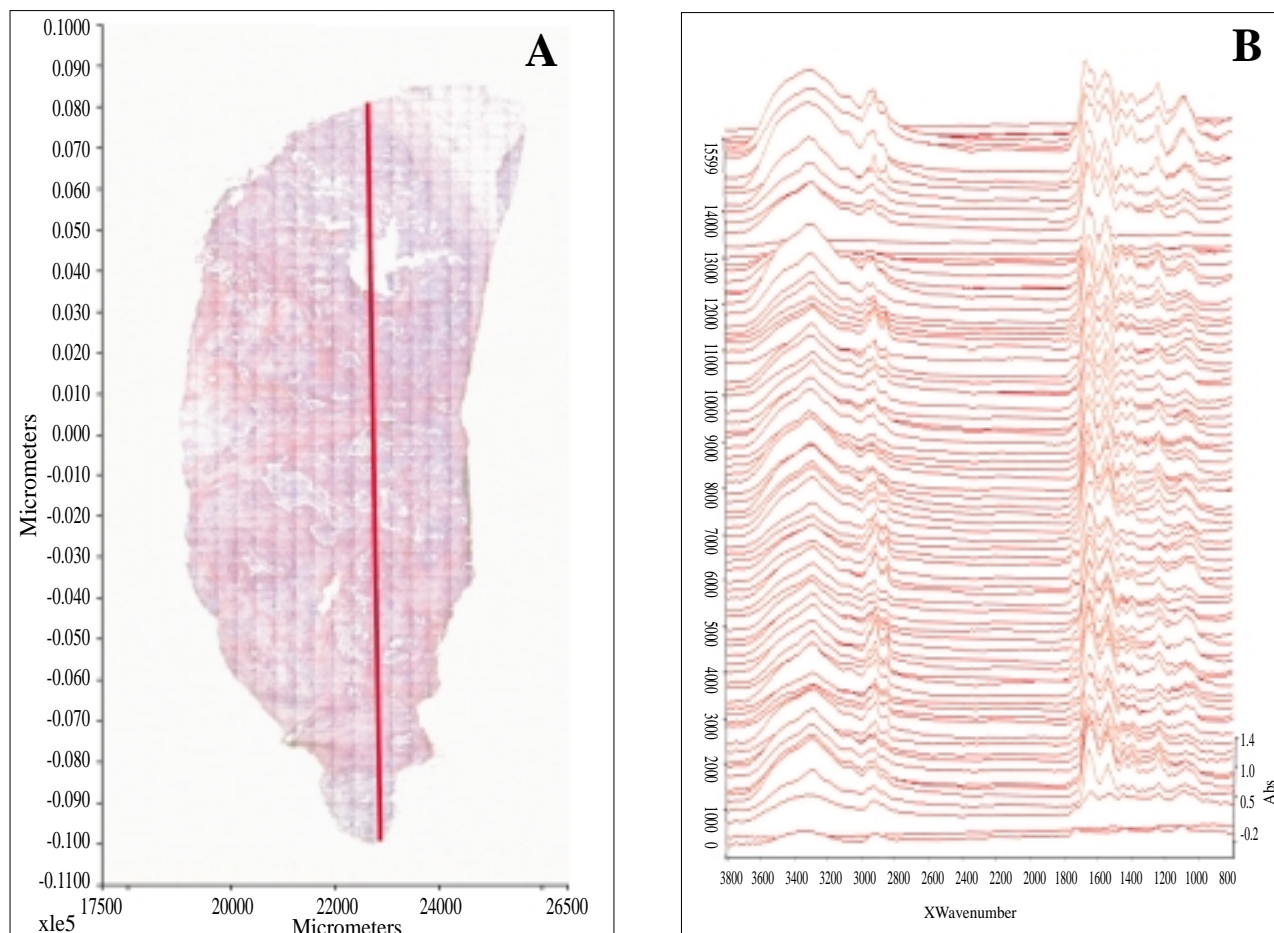


Fig. 2 FT-IR microscopic visible image of H & E stained human pancreatic cancer tissue (A) and the corresponding infrared line scanning spectra of unstained cancer tissue (B). The red line indicates the line scanning direction from bottom to top.

relative intensities, the numerous organic molecules present in cells produce spectra with complex, overlapping absorption bands. Rather than obtaining individual spectra, a piece of tissue cloud can be mapped via IR microspectroscopy, and then in a second step the entire area can be assessed for the biochemical distribution of components such as DNA, lipid or protein. These biochemical images reflect the cell component distribution, which could be correlated with stained tissue. This study conducted microscopic mapping of human pancreatic cancer tissue to obtain information on the spatial distribution of cancerous cells. Sample regions for the mapping were determined by examining an infrared microscopic field compared with corresponding photomicrographs, as shown in Fig. 3. Fig. 3C displays a typical infrared total absorbance map of pancreatic cancer

tissue, together with the unstained infrared visible image (Fig. 3B) and the corresponding H & E stained infrared visible image (Fig. 3A). Differences in the spectra were noted at the characteristic position of the amide I absorption region between 1700 and 1600 cm^{-1} (Fig. 1) which provided the most important source of protein secondary structural information.⁽¹²⁻¹⁴⁾ The protein conformational change of the cancer tissue could be expressed as the ratio of the absorbance wavenumber at 1659/1666, which represented the intensity of the amide I band of the cancerous and noncancerous tissue, respectively. The map in Fig. 3D reveals that the same color cluster provided a similar spectrum, and the lighter color cluster indicated the presence of more cancerous cells in the section.

The distribution pattern of the cancerous section

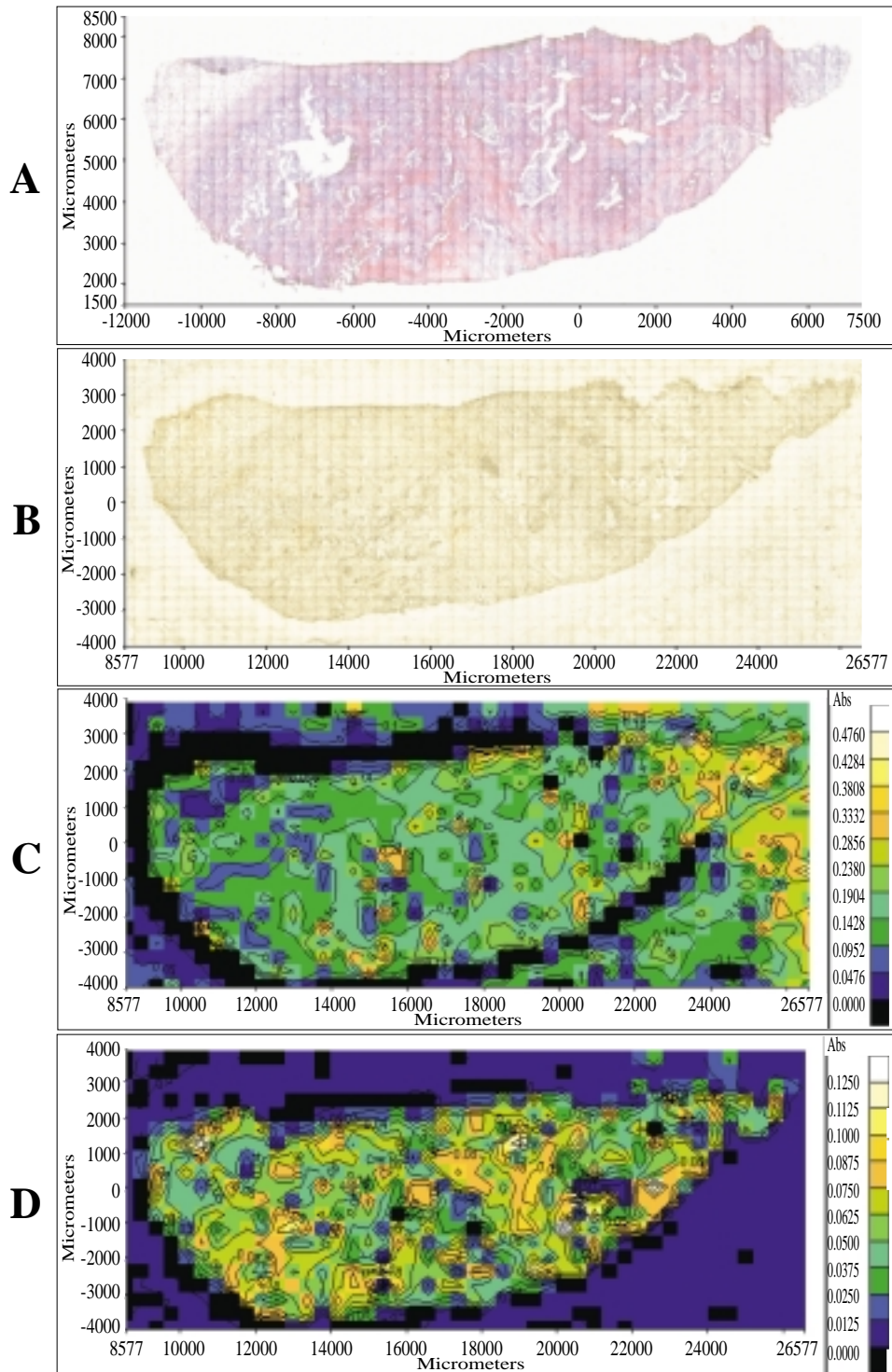


Fig. 3 Visible images using an FT-IR microscope and their corresponding maps of pancreatic cancer tissue. (A) infrared microscopic visible image of stained cancer tissue; (B) infrared microscopic visible image of the corresponding unstained cancer tissue; (C) total absorbance false color map with contours of the unstained cancer tissue; (D) false color map with contours of the 1659/1666 ratios in the unstained cancer tissue.

in the false color map with contours was almost identical to that in the corresponding photomicrograph of the cancer tissue, as shown in Fig. 3. Comparison of maps of different functional groups/ratios provided information on the relative distribution of materials within the sample. Fig. 4 illustrates the abnormal distributions of biochemical components within the cancerous tissue. Fig. 4A-4C display the false color functional group maps calculated from absorption bands at 2925, 1659, and 1084 cm^{-1} in cancerous tissue. Biochemical images were re-assembled based on specific marker bands. The lipid false color map, based on the CH_2 stretching absorption band at 2925 cm^{-1} indicated the lipid content in the cancerous tissue as shown in Fig. 4A. Meanwhile, Fig. 4B shows protein distribution throughout the section, based on the amide I band at 1659 cm^{-1} of protein. The cancerous tissue displayed significant protein content. The phosphodiester symmetric stretching vibration of nucleic acids at 1084 cm^{-1} was strong, and was used as an indicator of nucleic acid content. In the false color map in Fig. 4C, the DNA distribution was very low in the cancerous tissue, indicating low quantities of nucleic acids in the cancer tissue. Fig. 4D compares the different infrared spectra from the same color cluster of the lipids, proteins, and nucleic acids. These analytical results demonstrate that the false color maps reflect biochemical component changes in the spatial distribution of cancerous cells in human pancreatic tissue.

DISCUSSION

From the IR imaging maps, cancerous cells can be confirmed to be dispersed evenly in the light sections of tissues, and thus the spectra obtained from these places mostly result from the cancerous sections of protein. A significant protein content was noted in the cancerous tissue, reflecting the high levels of proteins in human pancreatic cancer tissue. The extent and local detectability of the IR spectral variations clearly are consistent with the known conformational change in protein. Thus, IR spectral changes provide a new biophysical parameter based on molecular markers indicating the spread of cancerous pathology in the pancreas. The content and distribution of lipid and DNA in the cancerous tissue were extremely low, indicating low levels of lipids

and nucleic acids in pancreatic cancer tissue. These measured results resemble the molecular alterations in pancreatic cancer tissue.⁽⁴⁾

The analytical results of this study demonstrate biochemical changes in the IR spectra of pancreatic cancer tissue, which can be used to distinguish between cancerous and noncancerous tissue. Similar analytical results were also found in other cancers including colorectal adenocarcinoma, breast cancer, skin tumors and lung cancer.^(10,11,18) The initially applied procedure included identification of structure-specific spectra from various absorption bands in the IR spectra and IR imaging, followed by extraction of these spectra for comparative purposes. Since one or more absorption bands correspond to the functional group characteristic for a class of molecules rather than for a single specific compound, and since spectral variations occur in various different absorption bands, superposition of multimolecular information can be concluded to be the basis of the disease-specific spectral changes. On the molecular level, the observed spectral differences are consistent with the identified phenotypic features. The IR absorbance for noncancerous tissue exceeds that of cancerous tissue in the human pancreas, similar to the literature spectra from several different tissues.⁽¹⁸⁾ Particularly, the frequency region of absorption bands at the amide bands and the CH_3 bending modes of methyl groups in proteins may indicate disorder of protein conformation in pancreatic cancer. The relative intensity changes of the bands CH_2 to CH_3 in the region from 3100 to 2800 cm^{-1} may also indicate lipid disorder in pancreatic cancer. Similar analytical results were observed in human gastric cancer, colon cancer, and prostate cancer tissues.^(17,19) Changes in the absorption bands at 1232, 1084, and 970 cm^{-1} containing contributions from nucleic acids owing to the ribose skeletal C-O-C and C-C stretching vibrations and P = O stretching vibrations may also indicate DNA or RNA changes resulting from DNA decomposition during apoptosis and/or a changed RNA content owing to upregulation or downregulation of genes.⁽²⁰⁾ The change in band shape at around 1232 and 1084 cm^{-1} , may also demonstrate an altered absorption of the ring vibration of carbohydrates, which could be assigned to the sugar moieties of nucleic acids, to changed content of metabolic sugar molecules in the cells, such as glucose, or to other as yet undescribed events.⁽²⁰⁾ The

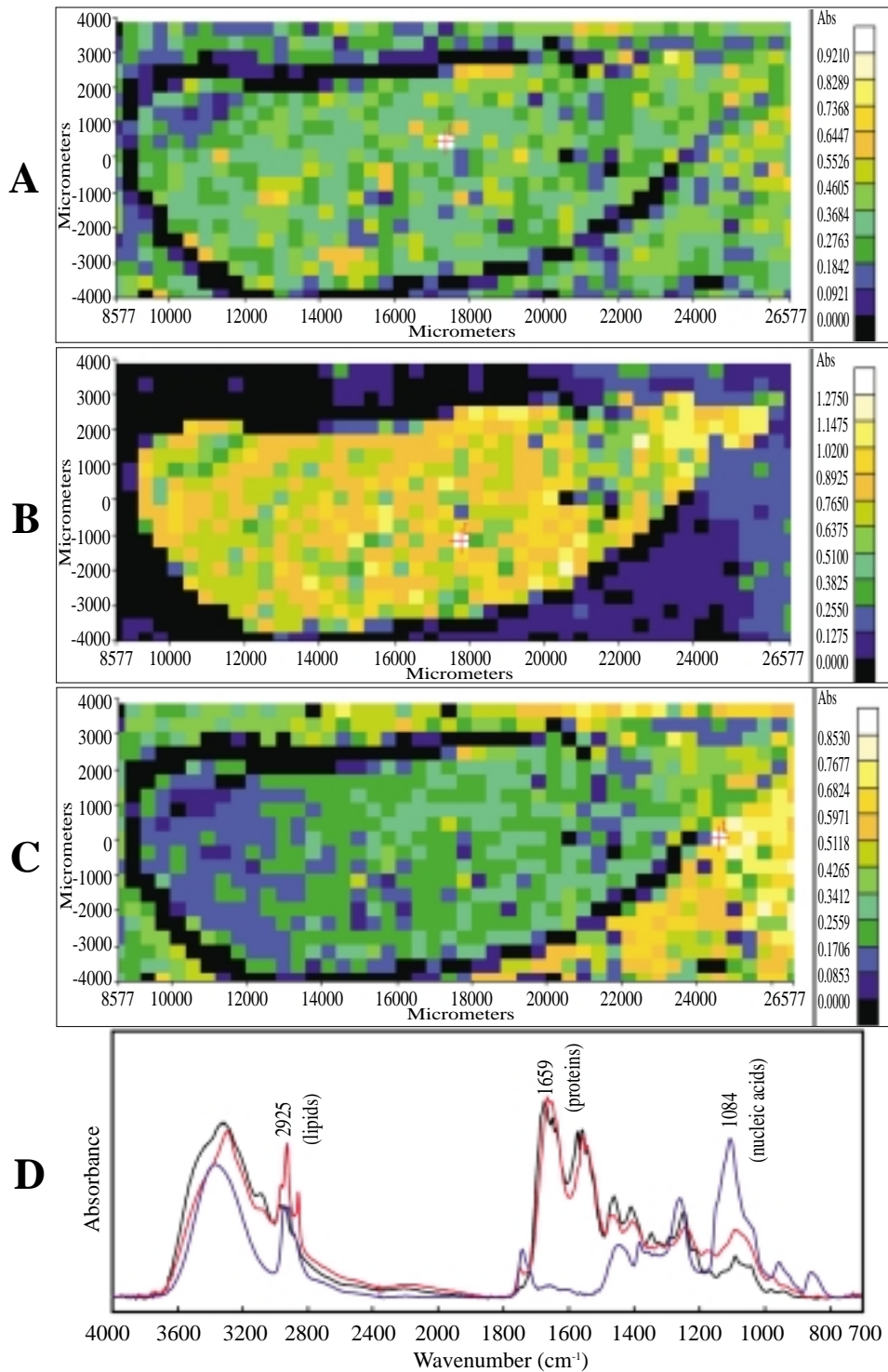


Fig. 4 Infrared biochemical mapping of pancreatic cancer tissue and the corresponding IR spectra. (A) false color functional group map from lipid absorption at 2925 cm^{-1} ; (B) false color functional group map from protein absorption at 1659 cm^{-1} ; (C) false color functional group map from nucleic acid absorption at 1084 cm^{-1} ; (D) comparison of different infrared spectra from the same color cluster of lipids (red line), proteins (black line), and nucleic acids (blue line). Red cross markers represent the IR spectra obtained from the false color functional maps of the lipids, proteins, and nucleic acids.

findings of spectral differences demonstrate that they clearly progress during the course of the cancer in the spectra. This phenomenon resembles the well-known spread of the histopathological features in pancreatic cancer.

This functional group mapping produces images of the chemical substructures and can be directly related to the microscope images of stained tissue sections. The present results indicate that sample information is contained in the infrared spectra of tissue materials and can be used to define different spectral patterns related to tissue biological structures. Functional group mapping provides spatial information based on absolute intensity or the relative material distribution. This study demonstrated a consistent link between cancerous tissue and various molecular changes, which can be detected via FT-IR spectroscopy *in situ* without prior staining. These analytical results indicate that FT-IR spectroscopy can accurately and rapidly detect adenocarcinoma in pancreatic tissues. This study using noncancerous and cancerous pancreatic tissue samples has clearly demonstrated that FT-IR microscopy can be developed for diagnostic purposes.

REFERENCES

- Jemal A, Tiwari RC, Murray T, Ghafoor A, Samuels A, Ward E, Feuer EJ, Thun MJ. American Cancer Society. Cancer statistics, 2004. *CA Cancer J Clin* 2004;54:8-29.
- Analysis of main causes of death in Taiwan for the year 2003, Department of Health, Executive Yuan, Taiwan, R.O.C. (2004)
- Williamson RC. Pancreatic cancer: the greatest oncological challenge. *Br Med J* 1988;296:445-6.
- Gold EB, Goldin SB. Epidemiology of and risk factors for pancreatic cancer. *Surg Oncol Clin N Am* 1998;7:67-91.
- Lucarotti ME, Habib NA, Kelly SB, Rothnie ND, Nelson O, Lindholm L, Cooper MJ, Wood CB, Williamson RC. Clinical evaluation of combined use of CE, CA19-9 and CA50 in the serum of patients with pancreatic carcinoma. *Eur J Surg Oncol* 1991;17:51-3.
- Jamin N, Dumas P, Moncuit J, Fridman WH, Teillaud JL, Carr GL, Williams GP. Highly resolved chemical imaging of living cells by using synchrotron infrared microspectrometry. *Proc Natl Acad Sci USA* 1998;95:4837-80.
- Jamin N, Dumas P, Moncuit J, Fridman WH, Teillaud JL, Carr GL, Williams GP. Chemical imaging of nucleic acids, proteins and lipids of a single living cell. Application of synchrotron infrared microspectrometry in cell biology. *Cell Mol Biol (Noisy-le-Grand)* 1998;44:9-13.
- Kalasinsky KS. Drug distribution in human hair by infrared microscopy. *Cell Mol Biol (Noisy-le-Grand)* 1998;44:81-7.
- Choo L, Wetzel DL, Halliday WC, Jackson M, Levine SM, Mantsch HH. In situ characterization of beta-amyloid in Alzheimer's diseased tissue by synchrotron Fourier transform infrared microspectroscopy. *Biophys J* 1996;71:1672-9.
- Wood BR, Chiriboga L, Yee H, Quinn MA, McNaughton D, Diem M. Fourier transform infrared (FTIR) spectral mapping of the cervical transformation zone, and dysplastic squamous epithelium. *Gynecol Oncol* 2004;93:59-68.
- Lasch P, Haensch W, Naumann D, Diem M. Imaging of colorectal adenocarcinoma using FT-IR microspectroscopy and cluster analysis. *Biochim Biophys Acta* 2004;1688:176-86.
- Cooper EA, Knutson K. Fourier transform infrared spectroscopy investigations of protein structure. In: Herron JN, Jiskoot W, Crommelin DJA, eds. *Physical Methods to Characterize Pharmaceutical Proteins*. New York: Plenum Press, 1995:101-43.
- Jackson M, Mantsch HH. Biomedical infrared spectroscopy. In: Mantsch HH, Chapman D, eds. *Infrared Spectroscopy of Biomolecules*. New York: Wiley-Liss, Inc., 1996:311-40.
- Naumann D. FT-Infrared and FT-Raman spectroscopy in biomedical research. In: Gremlich HU, Yan B, eds. *Infrared and Raman Spectroscopy of Biological Materials*. New York: Marcel Dekker, Inc., 2001:323-77.
- Kneipp J, Lasch P, Baldauf E, Beekes M, Naumann D. Detection of pathological molecular alterations in scrapie-infected hamster brain by Fourier transform infrared (FT-IR) spectroscopy. *Biochim Biophys Acta* 2000;1501:189-99.
- Meurens M, Wallon J, Tong J, Noel H, Haot J. Breast cancer detection by Fourier transform infrared spectrometry. *Vib Spectrosc* 1996;10:341-6.
- Rigas B, Wong PTT. Human colon adenocarcinoma cell lines display infrared spectroscopic feature of malignant colon tissues. *Cancer Res* 1992;52:84-8.
- Yano K, Ohoshima S, Gotou Y, Kumaido K, Moriguchi T, Katayama H. Direct measurement of human lung cancerous and noncancerous tissues by fourier transform infrared microscopy: can an infrared microscope be used as a clinical tool? *Anal Biochem*. 2000;287:218-25.
- Paluszkiwicz C, Kwiatek WM. Analysis of human cancer prostate tissues using FTIR microspectroscopy and SRIXE techniques. *J Mol Struc* 2001;565/566:329-34.
- Kneipp J, Beekes M, Lasch P, Naumann D. Molecular changes of preclinical scrapie can be detection by infrared spectroscopy. *J Neurosci* 2002;22:2989-97.

人類胰臟癌組織生物化學影像變化之紅外線光譜觀察

陳英仁 鄭奕帝¹ 劉欣怡² 林博彥³ 王嘉修⁴

傅立葉紅外線 (FT-IR) 顯微光譜的圖像化技術可以被用來區別組織結構間的不同形態，並且可以增加被測組織樣品的正常及癌化部分之影像對比。本研究係利用傅立葉紅外線圖像化方法來描述於人類胰臟癌組織紅外光譜上介於癌組織與不同分子變化間的生物化學變化之相關連性研究。由進行末端胰體部與尾部切除術之胰臟癌病人身上切取腫瘤部位組織以供研究用。在本研究中我們利用傅立葉紅外線顯微光譜結合影像化、圖像化及線掃描技術來進行人類胰臟癌組織之脂質、蛋白質及核甘酸的生物化學影像變化研究。人類胰臟癌組織之紅外線光譜的吸收強度及吸收頻率戲劇性地被降低及位移，特別是在蛋白質的醯胺鍵及脂質的 CH₂ 與 CH₃ 鍵伸縮震動。在人類胰臟癌組織可發現明顯的蛋白質含量，而且亦可發現癌組織中 DNA 及脂質的分布含量很少，而這指出核甘酸與脂質在人類胰臟癌組織中含量很低。這些分析結果指出傅立葉紅外線顯微光譜的生物化學影像反映出細胞成分的分布，而這與胰臟組織的腺癌染色組織具相關連性。我們的非癌化與癌化胰臟組織樣品之研究已經很明顯地指出，傅立葉紅外線顯微光譜結合影像化的方法可被用來當作診斷之用。(長庚醫誌 2006;29:518-27)

關鍵字：胰臟癌，生物化學影像，圖像化，紅外線顯微光譜。

長庚紀念醫院 林口院區 一般內科；長庚紀念醫院 嘉義院區 ¹藥劑科，²護理部，³病理科，⁴外科部

受文日期：民國93年4月30日；接受刊載：民國94年10月17日

索取抽印本處：鄭奕帝主任，長庚紀念醫院 藥劑科。嘉義縣613朴子市嘉朴路西段6號。Tel.: (05)3621000轉2152; Fax: (05)3623002; E-mail: phdcheng@cgmh.org.tw